Published in final edited form as:
Int J Neuropsychopharmacol. 2011 October ; 14(9): 1219–1232. doi:10.1017/S1461145710001525.

Chronic desipramine treatment alters tyrosine hydroxylase but not norepinephrine transporter immunoreactivity in norepinephrine axons in the rat prefrontal cortex

Susan L. Erickson[1], **Anjalika R. Gandhi**[1], **Josephine K. Asafu-Adjei**[2], **Allan R. Sampson**[2], **LeeAnn Miner**[1], **Randy D. Blakely**[3], and **Susan R. Sesack**[1,4,*]

[1]Department of Neuroscience, University of Pittsburgh, Pittsburgh, PA 15260

[2]Department of Statistics, University of Pittsburgh, Pittsburgh, PA 15260

[3]Department of Pharmacology, School of Medicine, and Center for Molecular Neuroscience, Vanderbilt University, Nashville, TN 37232

[4]Department of Psychiatry, University of Pittsburgh, Pittsburgh, PA 15260

Abstract

Pharmacological blockade of norepinephrine (NE) reuptake is clinically effective in treating several mental disorders. Drugs that bind to the NE transporter (NET) alter both protein levels and activity of NET and also the catecholamine synthetic enzyme tyrosine hydroxylase (TH). We examined the rat prefrontal cortex (PFC) by electron microscopy to determine whether the density and subcellular distribution of immunolabeling for NET and colocalization of NET with TH within individual NE axons were altered by chronic treatment with the selective NE uptake inhibitor desipramine (DMI). Following DMI treatment (21 days, 15 mg/kg/day), NET-immunoreactive (-ir) axons were significantly less likely to colocalize TH. This finding is consistent with reports of reduced TH levels and activity in the locus coeruleus after chronic DMI and indicates a reduction of NE synthetic capacity in the PFC. Measures of NET expression and membrane localization, including the number of NET-ir profiles per tissue area sampled, the number of gold particles per NET-ir profile area, and the proportion of gold particles associated with the plasma membrane, were similar in DMI and vehicle treated rats. These findings were verified using two different antibodies directed against distinct epitopes of the NET protein. The results suggest that chronic DMI treatment does not reduce NET expression within individual NE axons in vivo or induce an overall translocation of NET protein away from the plasma membrane in the PFC as measured by ultrastructural immunogold labeling. Our findings encourage consideration of possible postranslational mechanisms for regulating NET activity in antidepressant-induced modulation of NE clearance.

Keywords

antidepressant; anatomy; electron microscopy; SNRI

Correspondence: Susan R. Sesack, PhD, A210 Langley Hall, University of Pittsburgh, Pittsburgh, PA 15260, Phone: 412-624-5158, Fax: 412-624-9198, sesack@pitt.edu.

STATEMENT OF INTEREST: The Authors declare no conflict of interest.

Introduction

The prefrontal cortex (PFC) is a critical regulator of higher cognitive functions and affective state. Dysfunction of the PFC is implicated in numerous psychiatric illnesses, including depression, attention deficit disorder and post traumatic stress disorder (DeRubeis et al., 2008; Drevets et al., 1992; Ernst et al., 1994; Huey et al., 2008; Mostofsky et al., 2002; Rauch et al., 2003; Ressler and Mayberg 2007; Soares and Mann 1997; Solanto 1998; Zametkin et al., 1990). Brainstem monoamine inputs play critical roles in regulating normative PFC operations, and disruption of the spatial and temporal integrity of monoamine transmission is hypothesized to contribute to PFC dysfunction (Aston-Jones et al., 1994; Bremner et al., 1996; Briand et al., 2007; Callado et al., 1998; Charney et al., 1995; Meana et al., 1992; Moreira 2007; Pliszka et al., 1996; Ramos and Arnsten 2007; Russell et al., 2000; Solanto 1998).

A critical link between monoamine signaling and PFC function is established by the clinical efficacy of drugs that block the reuptake of norepinephrine (NE) and/or serotonin through their respective transporters, i.e., NET and SERT (Bymaster et al., 2002; Frazer 2000; Kent 2000; Michelson et al., 2003; Moller 2000; Nelson 1999; Spencer et al., 2002). Chronic blockade of the NET with DMI causes an increase in extracellular NE in the PFC, concomitant with a decrease in total NE tissue content and a reduction in locus coeruleus (LC) neuronal activity (Grant and Weiss 2001; Huang et al., 1980; McMillen et al., 1980; Svensson and Udin 1978). These findings suggest an overall decrease in NE synthesis, which is further supported by reductions of tyrosine hydroxylase (TH) protein levels and synthetic activity in the LC following chronic antidepressant administration (Komori et al., 1992; Nestler et al., 1990; Zhu et al., 2005). The effect of DMI on TH protein levels could be compartment specific, but no study has directly assessed the effect of chronic DMI on the presence of TH protein in individual NE axon terminals in the PFC.

In contrast to consistent findings showing reduced transmitter synthesis, the effect of antidepressant treatment on the NET protein itself has produced variable results for measures of ligand binding, transmitter uptake and transporter detectability by immunoblot (Bauer and Tejani-Butt 1992; Benmansour et al., 2004; Galli et al., 1995; Hebert et al., 2001; Jeannotte et al., 2009; Ordway et al., 2005; Song et al., 2008; Weinshenker et al., 2002; Zhao et al., 2008; Zhu et al., 1998; Zhu et al., 2002; Zhu and Ordway 1997). Moreover, no study to date has examined NET protein within individual axon terminals or its localization to the plasma membrane in intact animals exposed to chronic NET blockade. In this study, we sought to apply an ultrastructural approach to address these questions. We hypothesized that chronic blockade of the NET with DMI would reduce both the overall density and membrane localization of NET in the PFC. Analyzing tissue dually labeled for NET and TH, we further hypothesized that chronic DMI would decrease the percentage of NE axons expressing detectable TH immunoreactivity in the PFC.

Methods

Animals

A total of 42 adult male Sprague Dawley rats (Hilltop Lab Animals, Scottsdale, PA) weighing 250-300 g were used in this study. Thirty rats were treated with DMI or vehicle, and twelve were used to determine optimal parameters for immunoreactivity (see Supplemental Material). The 30 rats treated with DMI or vehicle were processed and sacrificed in cohorts of 4 or 6, including 2 or 4 rats treated with DMI and 2 treated with vehicle. There were some differences between cohorts in animal handling, surgical procedures and tissue preparation, and so cohort was entered as a fixed factor in our statistical analyses (see Supplementary Material). However, within a cohort, animals

differed only with regard to drug exposure, and all tissue sections were processed together. If the plasma levels of DMI for all drug treated rats in a cohort were outside of the desired range (see below), the entire cohort (including controls) was dropped from the study. A total of 10 drug treated rats from five cohorts had satisfactory plasma DMI levels at the time of sacrifice. These and 10 vehicle treated rats from the same five cohorts were included in this study (Table 1).

All rats were single-housed (Benmansour et al., 1999) and maintained on a 12/12 hour light/dark cycle (lights on 0700) with *ad libitum* access to food and water. The experiments were conducted in accordance with animal use protocols approved by the University of Pittsburgh Institutional Laboratory Animal Care and Use Committee.

Chronic drug treatment

DMI or vehicle was administered to rats for 21 days via osmotic minipumps (model 2ML4, Alzet, Palo Alto, California). DMI was dissolved in 10% ethanol (Bondi et al., 2007; Garcia et al., 2004; Lapiz et al., 2007a; Lapiz et al., 2007b) and loaded into minipumps under sterile conditions. The dosage (15 mg/kg/d, free base) was selected based on published findings that this dose yields serum levels approximating those associated with therapeutic antidepressant actions in humans (120-600 ng/ml) (Benmansour et al., 1999). We also tried a lower dose in two rats (7.5 mg/kg/d; (Lapiz et al., 2007a), but in our hands this yielded plasma levels below the desired range.

Surgical procedures

For all cohorts except one, minipumps were placed intraperitoneally (i.p.; (Bondi et al., 2007; Lapiz et al., 2007a) under isoflurane anesthesia (2% in 95% O_2). All rats received penicillin (180,000 units) at the end of surgery, and again 2 and 4 days later. Rats were handled 2-3 times per week for weighing.

In the other cohort of rats, the minipumps were placed subcutaneously (s.c.) (Benmansour et al., 2004; Garcia et al., 2004; Lapiz et al., 2007b). In these rats, there was substantial buildup of connective tissue around the outlets of the minipumps containing DMI, and a large amount of fluid accumulated around the pump. The drug- and vehicle treated rats in this cohort were handled once or twice daily to manipulate the pump and free any connective tissue buildup. In addition, all of the drug- and vehicle treated rats in this cohort underwent a second surgery approximately halfway through the 21 day treatment period to either move the pump to the contralateral side or to drain the accumulated fluid. Switching to i.p. implantation for the remaining cohorts reduced the pain and stress exposure associated with the second survival surgery and daily manipulations and was a significant improvement in the protocol. Nevertheless, the first cohort was retained in the analysis because it included appropriate controls that were treated identically except for drug condition, and because statistical analyses included cohort as a fixed effect. Importantly, the plasma DMI levels from the rats with s.c. administration did not differ significantly from those receiving i.p. DMI.

At the time of sacrifice there were no obvious differences in the appearance of the DMI and vehicle treated animals. Most DMI treated rats gained weight more slowly than controls during the three week treatment period. However, the final percent increase in weight was not statistically different between the two groups ($t = 1.27$, $P = 0.12$).

Pumps were left in place for 21 days until the rats were killed at the end of the treatment period with no washout. Plasma DMI levels were determined from blood samples collected just prior to perfusion and assayed by Dr. Martin Javors, Department of Psychiatry, University of Texas Health Science Center at San Antonio.

Rats were anesthetized with Nembutal and transcardially perfused with 3.75% acrolein in 2% paraformaldehyde. Coronal sections (50 μm) were processed for immunocytochemistry (see Supplementary Material). At this point, all specimens were coded, and the remaining tissue processing and electron microscopic sampling were conducted with the experimenter blinded to treatment condition.

Immunocytochemistry

To address potential concerns about epitope availability in the NET protein after DMI treatment, two different anti-NET primary antibodies were used. Tissue from three cohorts of rats (A, B and C) was labeled with a rabbit polyclonal anti-NET antibody (1:1000 – 1:2000) directed at amino acids 585-607 of the C-terminus of the mouse NET protein. Specificity of this antibody was demonstrated by Western blot analysis and by the absence of staining in sections from mice with a transgenic deletion of the NET gene (NET-KO; (Fritz et al., 1998; Miner et al., 2006; Miner et al., 2003; Schroeter et al., 2000). Tissue from two cohorts of rats (D and E) was labeled with a monoclonal mouse anti-NET primary (1:250) directed against amino acid sequence 5-17 of the N-terminus of mouse NET (NET-05; (Matthies et al., 2009). Specificity of this antibody has been demonstrated by absence of immunolabeling in NET-KO tissue and following preadsorption with the antigenic peptide (Matthies et al., 2009). Sections labeled with the rabbit anti-NET antibody were also labeled with a commercially available mouse anti-TH primary antibody (1:4000; Millipore, Billerica, MA). Specificity of the latter antibody was demonstrated by Western blot analysis and radioactive immunoassay as described in previous publications (Sesack et al., 1995; Steinbusch et al., 1987; Wolf et al., 1991).

Sections were pretreated in a blocking solution containing bovine serum albumin (1%), and normal goat serum (3%) in tris buffered saline with either low (0.04%) or high (0.2%) Triton X-100 for electron or light microscopy, respectively. Sections were transferred into blocking solutions containing the primary antibodies and incubated overnight. Sections were then processed for immunoperoxidase or immunogold-silver and embedded in epoxy resin (see Supplementary Materials and Methods).

Small pieces of the prelimbic PFC (Krettek and Price 1977) were trimmed into trapezoids containing the superficial (I-III) or deep (V-VI) layers. Ultrathin (70 nm) sections were cut using an ultramicrotome and collected onto grids, counterstained, and examined with a transmission electron microscope. Digital photomicrographs were adjusted for brightness and contrast using Adobe Photoshop.

Tissue sampling

For each animal, two blocks each from the superficial and deep cortical layers were sampled. Grid squares at the tissue surface (i.e. containing a mix of tissue and plastic embedding material) were systematically examined at 22,000 X magnification until approximately 25 NET-immunoreactive (-ir) profiles were photographed for each block. The estimated total amount of tissue examined and the number of NET-ir profiles for each animal is listed in Table 1. NET-ir profiles were defined as axons containing at least two gold particles on the plasma membrane or at least three total gold particles. Gold particles that were clumped together with no light pixels between them were counted as one.

For every NET-ir profile, we counted all gold particles and assigned them to the membrane (if there were no light pixels between the membrane and the gold particle) or to the cytoplasm. The area and perimeter of each NET-ir profile were measured with SimplePCI software (Hamamatsu Corporation, Sewickley, PA). Synapses, if present, were categorized as symmetric (thin or absent postsynaptic density) or asymmetric (well defined postsynaptic

density) and by postsynaptic target (spine, dendritic shaft or soma). For tissue double-labeled for TH, we also noted the presence or absence of immunoperoxidase label for TH within the NET-ir profiles.

Ultimately, tissue was analyzed for 1) number of NET-ir profiles per unit tissue area sampled, 2) number of gold particles per unit profile area, 3) number of membrane-bound gold particles per unit profile perimeter, 4) percent of total gold particles associated with the plasma membrane, 5) percent of NET-ir profiles that formed synapses, and 6) percent of NET-ir profiles that contained detectable TH immunoreactivity (for the tissue double-labeled for TH).

The analyses of all six dependent measures were implemented in SAS PROC MIXED (Version 9.2, SAS Institute Inc., Cary, NC). All statistical tests were two sided and conducted at the 0.05 significance level. Statistical analysis revealed no significant differences between the superficial and deep layers in any measures of interest, so these data were combined for each animal in the presentation of the Results. Details of the statistical models are included in Supplementary Material.

Results

Light and electron microscopic examination of PFC NE axons after chronic DMI treatment

Within the medial PFC of control rats, the morphology and light microscopic distribution of NE axons labeled with either the mouse (Fig. 1A) or the rabbit anti-NET antibody (Fig. S1) matched our prior descriptions (Miner et al., 2006;Miner et al., 2003). Immunoperoxidase labeling revealed NET-ir axons throughout all layers of the prelimbic PFC, with an especially dense fiber plexus in the deep portion of layer 1. Labeled axons were relatively smooth and branched frequently. The orientation of NET-ir fibers was predominantly tangential in layers 1 and 6, and relatively radial in the middle layers. The laminar pattern and density of NE axons labeled by immunoperoxidase for NET were qualitatively similar in the DMI treated versus control rats using either the mouse (Fig. 1B) or the rabbit anti-NET antibody (not shown).

Immunogold-silver staining of NET in the PFC of control rats using the mouse primary antibody (Fig. 2) revealed specific labeling of both small diameter axons consistent with fibers of passage, and larger profiles consistent with varicosities, as described previously (Miner et al., 2006;Miner et al., 2003). Synaptic vesicles were observed in all large and some small NET-ir axons. NET-ir varicosities occasionally formed synapses (Fig. 2 E, F). The subcellular distribution of immunogold-silver labeling for NET varied from most or all on the plasma membrane (Fig. 2A-C), most or all in the cytoplasm (Fig. 2D), or a mix of plasmalemmal and cytoplasmic label (Fig. 2 E, F). In DMI treated rats, immunogold-silver labeling of NET was qualitatively indistinguishable from vehicle treated controls in size, density of NET labeling, and the proportion of plasmalemmal to cytoplasmic NET particles (Fig. 3).

Quantitative measures of NET immunoreactivity in DMI and vehicle treated rats

Figure 4 shows the number of NET-ir profiles observed per 1,000 μm^2 of tissue examined for each animal in the DMI and vehicle treated groups. We found no significant main effect of chronic DMI treatment on the density of NET-ir profiles ($F_{(1, 13.6)} = 0.06$, $p = 0.81$; please see Table 2 for related confidence limits). Furthermore, the density of NET-labeled profiles showed no correlation to plasma DMI levels (Table 1). As expected, we did observe a significant effect of cohort on the density of NET-ir profiles, although the values for the DMI and vehicle treated rats were consistently similar within each cohort. Of the 1217 NET-ir profiles sampled from the control group, 571 (47%) met the minimum inclusion criterion,

whereas the rest exceeded the criterion. From the 1170 NET-ir profiles in the DMI group, 429 (37%) met the minimum criterion. The size of the NET-ir profiles was similar in the vehicle and DMI treated animals: 0.38 +/- 0.09 μm^2 (mean +/- stdev) versus 0.39 +/- 0.10 μm^2, respectively.

Figure 5 shows the effect of DMI treatment on three measures of immunogold-silver labeling for individual NET-ir profiles in each animal. Chronic treatment with DMI had no significant effect on the number of gold particles per unit profile area ($F_{(1, 13.8)} = 0.01$, $p = 0.91$; Fig. 5A), the number of membrane-bound gold particles per unit profile perimeter ($F_{(1, 13.3)} = 0.01$, $p = 0.93$; Fig. 5B) or the percentage of total gold particles associated with the plasma membrane ($F_{(1, 13.8)} = 1.13$, $p = 0.30$; Fig. 5C; see Table 2 for related confidence limits). We observed significant cohort effects for the number of gold particles per unit profile area and the number of membrane-bound particles per unit profile perimeter. Nevertheless the values for DMI- or vehicle treated rats were consistently similar within each cohort. For the number of membrane-bound gold particles per unit profile perimeter, there was a significant fixed effect of the number of gold particles per unit profile area ($F_{(1, 57)} = 136.10$, $p < 0.0001$), suggesting that the main contributing factor to membrane gold density was the overall gold density.

DMI treatment did not affect the incidence of synapses observed in this single section analysis (Table 3). We did observe a significant main effect of antibody on synaptic incidence ($F_{(1, 14.3)} = 8.04$, $p = 0.01$). We note that the tissue prepared with the rabbit anti-NET antibody was dually labeled with immunoperoxidase for TH, and the presence of peroxidase product may have obscured synaptic specializations. When we analyzed just the single-labeled NET-ir profiles from the double-labeled tissue, the synaptic incidence was comparable to the material prepared with the mouse anti-NET antibody.

TH immunoreactivity in NET-ir profiles in DMI and vehicle treated rats

In the three cohorts of rats where sections were dually labeled for NET and TH, 32% of the NET-ir profiles contained detectable TH labeling in the DMI treated rats compared to 48% in the controls. This reduction in TH expression was statistically significant ($F_{(1, 7.25)} = 6.15$, $p = 0.04$; Fig. 6). The morphological features of the dually-labeled NET- and TH-ir profiles in both treatment groups (Fig. 7) generally resembled those of the single labeled NET-ir profiles, with two exceptions. First, the percent of gold particles associated with the plasma membrane was consistently higher in the double-labeled terminals compared to the singly-labeled NET-ir terminals, consistent with our previous reports (Miner et al., 2006;Miner et al., 2003). Second, the incidence of synapses was markedly lower in the dually-labeled profiles (see above), also consistent with prior data. However, there was no effect of DMI treatment evident in these measures.

Discussion

In this first ultrastructural study of its kind, we showed that chronic DMI treatment was associated with a significant reduction in the percentage of NET-ir terminals expressing detectable TH but had no measurable effect on NET protein expression in the intact rat PFC. Both the number of NET-ir axons per unit area sampled and the number of gold particles per profile area were similar in DMI treated animals and controls. In addition, the subcellular localization of NET was unaffected by DMI administration, in that approximately half of immunogold particles were associated with the plasma membrane of NET-ir axons in both treatment groups. These findings were consistent using two different antibodies directed against different intracellular epitopes of the NET protein. These results have important implications for understanding how NE transmission in the PFC adapts to chronic blockade of the NET.

Methodological considerations

Sampling—We did not use unbiased stereological methods of sampling in this study. However, we did note that the mean size of NET-ir profiles, a major source of sampling bias, did not differ between the DMI and vehicle treated rats. Therefore, a difference in profile size in the two treatment groups was not a source of bias in this study.

Sensitivity—In our ultrastructural analysis, a decrease in the total amount of NET protein after DMI would have been evident in at least one of two measures: the total number of gold particles per unit profile area, or the total number of NET-ir profiles per unit tissue area sampled. We considered whether our criteria for inclusion of NET-ir axons (i.e., two membrane gold particles, or three total) may have limited our ability to detect a significant DMI related decrease in the density of gold labeling within individual profiles because the loss of just one gold particle from each profile would have resulted in close to half of the population dropping below our inclusion criterion. However, the fact that we did not detect a change in the number of NET-ir profiles per area sampled in the DMI treated animals suggests that this did not happen.

Two additional lines of evidence suggest that changes in overall protein expression and membrane localization can be detected with this assay. First, this approach has been clearly established as sufficient to demonstrate acute relocalization of membrane proteins following pharmacological and environmental manipulation (Dumartin et al., 1998; Glass et al., 2004; Hara and Pickel 2007; Riad et al., 2001). Second, we have previously shown both that chronic exposure to sertraline or chronic stress can induce significant changes in immunogold labeling of the serotonin transporter and of NET, respectively (Miner et al., 2004; Miner et al., 2006). These observations support the conclusion that changes in NET expression are detectable with immunogold labeling, and the lack of alterations in NET following chronic DMI are not due to limited sensitivity of the labeling method.

TH expression

Ours is the first study to selectively assess the impact of chronic antidepressant treatment on the presence of TH in individual, positively identified NE terminals remote from the LC. Only one previous study assessed TH levels in an NE terminal field after antidepressant treatment, but interpretation of the findings was complicated by the inclusion of dopaminergic axons (Zhu et al., 2005). Our observation that DMI treatment significantly reduced the percentage of NET-ir terminals that also contained detectable TH was not unexpected, given that multiple studies have shown that chronic DMI treatment causes a decrease of about 50% in TH protein levels in samples containing NE somata (Komori et al., 1992; Nestler et al., 1990; Zhu et al., 2005). The present finding confirms that TH protein in the PFC terminal field is regulated in concert with the cell body. TH levels in NE neurons are increased in major depression, and whether this reflects primary overactivity of the NE system in the pathophysiology of the disorder or a compensatory measure responding to NE deficiency remains unclear (Zhu et al., 1999). In either case, it is not surprising that a change induced by antidepressant treatment would be in the opposite direction.

NET expression

Although previous studies in cultured cells have consistently reported a downregulation of NET following DMI exposure (Zhu et al., 1998; Zhu and Ordway 1997), studies in intact animals have produced mixed results. Several studies have shown that chronic DMI treatment resulted in no effect on measures of NET expression in the cortex (Bauer and Tejani-Butt 1992; Hebert et al., 2001; Song et al., 2008), while others reported reductions of NET expression ranging from 22-50% (Benmansour et al., 2004; Zhao et al., 2008). Differences in experimental design (drug dose, delivery route, treatment duration and NET

assay method) may explain some of these disparities. In our study, the lower limits of the 95% confidence intervals indicate that the largest reductions in NET expression consistent with observed results are on the order of 12-21%. Although we cannot rule out DMI effects of very small magnitude, we note that no previous study has reported significant effects smaller than 20%.

One aspect of our experiment complicates comparison to previous studies is the lack of a washout period. Earlier reports state that after discontinuation of chronic, systemic treatment, serum levels of DMI require 72 hours to fall below 5 ng/ml (Benmansour et al., 1999). Therefore, reducing residual drug with a washout period is critical for assays that rely on accessible radioligand or substrate binding sites. However, implementing a washout has several drawbacks. First, removal of the minipumps requires subjecting the rats to a second survival surgery. This major stressor causes the animals discomfort, and exposure to stress could impact our results (Miner et al., 2006). Second, as the plasma levels of drug decline, compensatory adjustments in various measures of NET expression, including membrane localization, could occur, and this too could potentially impact our finding. Zhao et al. (Zhao et al., 2008) noted that NET protein levels change gradually after discontinuing DMI treatment, and took eight days to return to control levels. Thus, any assays performed two days after treatment might not yield results identical to those obtained during drug exposure. For immunocytochemical detection, the hypothesized location of the DMI binding site on the NET indicates that residual drug would be unlikely to interfere with antibody binding. Moreover, our assay utilized two different primary antibodies directed at different intracellular epitopes of NET that were not expected to be obscured by residual DMI or conformational changes associated with bound drug (Singh et al., 2007; Zhou et al., 2007). Consequently, a washout period was deemed unnecessary and potentially deleterious. Finally, we believe that the washout period is unlikely to account for our negative outcome, given that previous studies using a washout period reported both positive and negative findings.

Subcellular localization of NET

Our methods of immunogold labeling and electron microscopic sampling are well suited to assessing the subcellular localization of monoamine transporters (Miner et al., 2006; Miner et al., 2000; 2003). A previous preliminary report from this laboratory demonstrated that chronic sertraline exposure caused a modest but significant reduction in membrane-associated SERT immunoreactivity in the rat PFC (Miner et al., 2004). Similar to the mixed outcomes of experiments assaying total NET protein, previous studies have also yielded inconsistent results when measuring the level of membrane-bound NET after systemic DMI. Jeannotte and colleagues (Jeannotte et al., 2009) reported that the proportion of total NET associated with the membrane compartment in frontal cortex was similar in DMI and vehicle treated animals. In contrast, Song et al. (Song et al., 2008) reported a decrease of more than 50% in the amount of NET protein contained in cell surface fractions from the hippocampus after DMI treatment. Our present findings agree with the former study in frontal cortex, and suggest that chronic DMI did not induce substantial amounts of NET to traffic away from the plasmalemma in the PFC. It would be interesting to examine the hippocampus in future ultrastructural studies to determine whether chronic DMI induces a significant change in membrane NET in that region.

Reduced uptake activity in the absence of changes in protein levels or membrane trafficking might be explained by catalytic modifications of NET. For example, adenosine receptor stimulation alters SERT function both by influencing surface translocation and by augmenting intrinsic activity through a p38 mitogen activated protein kinase dependent mechanism (Zhu et al., 2004). A similar phenomenon appears to underlie the insulin activation of NET protein already expressed on the cell surface (Apparsundaram et al.,

2001). Recent evidence suggests that a similar augmentation of intrinsic NET activity occurs in association with genetically-induced decreased NET expression (M. Hahn, personal communication). Whether such trafficking-independent regulatory mechanisms contribute to alterations in NET uptake capacity or possible therapeutic actions in the presence of chronic DMI remains to be explored.

Functional implications

Chronic treatment with tricyclic antidepressants has been shown to reduce both the spontaneous and evoked activity of LC neurons, and cellular activity is one of the factors regulating the surface distribution of NET (Grant and Weiss 2001; Savchenko et al., 2003; Szabo and Blier 2001). We previously hypothesized that elevated membrane localization of NET together with the presence of detectable TH could represent a heightened “activity state” of NE terminals (Miner and Sesack; Miner et al., 2006). Based on the physiological response of NE cells to antidepressants, we therefore predicted that chronic DMI would induce the morphological characteristics associated with a lowered activity state (i.e., reduced plasmalemmal NET and TH). The fact that we only observed a reduction in detectable TH suggests that other factors besides cellular activity control the degree of membrane distribution of NET. Indeed, it may be possible that there is a physiologically determined lower limit of NET that must be expressed on the plasma membrane, such that antidepressant treatment cannot reduce this further, at least as measured by electron microscopic immunogold labeling.

We previously demonstrated that chronic stress, a proposed animal model of depression, increases plasmalemmal NET localization (Miner et al., 2006). Although we report here that DMI treatment by itself did not shift a significant proportion of NET off the plasma membrane, it should be noted that these were otherwise naïve rats, making it possible that DMI treatment might yet demonstrate effects on NET distribution in animals undergoing environmental manipulations such as stress. Hence, DMI administration to naïve rats might not adequately reflect the effect of treatment in stressed or depressed individuals. Further studies are needed to test the ability of chronic DMI treatment to prevent the chronic-stress induced enhancement of NET distribution to the plasma membrane.

Supplementary Material

Refer to Web version on PubMed Central for supplementary material.

Acknowledgments

This work was supported by NIH Grants MH074700 (S.R.S.) and MH058921 (R.D.B).

References

Apparsundaram S, Sung U, Price RD, Blakely RD. Trafficking-dependent and -independent pathways of neurotransmitter transporter regulation differentially involving p38 mitogen-activated protein kinase revealed in studies of insulin modulation of norepinephrine transport in SK-N-SH cells. Journal of Pharmacology and Experimental Therapeutics. 2001; 299:666–677. [PubMed: 11602680]

Aston-Jones, G.; Valentino, R.; VanBockstaele, E.; Meyerson, A. Locus coeruleus, stress, and PTSD: neurbiological and clinical paralles. In: Murbur, M., editor. Catecholamine Function in PTSD: Emerging Concepts. Washington, DC: American Psychiatric Press; 1994. p. 17-62.

Bauer M, Tejani-Butt S. Effects of repeated administration of desipramine or electroconvulsive shock on norepinephrine uptake sites measured by [3H]nisoxetine autoradiography. Brain Research. 1992; 582:208–214. [PubMed: 1327403]

Benmansour S, Altamirano A, Jones D, Sanchez T, et al. Regulation of the norepinephrine transporter by chronic administration of antidepressants. Biological Psychiatry. 2004; 55:313–316. [PubMed: 14744474]

Benmansour S, Cecchi M, Morilak DA, Gerhardt GA, et al. Effects of chronic antidepressant treatments on serotonin transporter function, density, and mRNA level. Journal of Neuroscience. 1999; 19:10494–10501. [PubMed: 10575045]

Bondi CO, Barrera G, Lapiz MD, Bedard T, et al. Noradrenergic facilitation of shock-probe defensive burying in lateral septum of rats, and modulation by chronic treatment with desipramine. Progress in Neuropsychopharmacology and Biological Psychiatry. 2007; 31:482–495.

Bremner J, Krystal K, Soutwick S, Charney D. Noradrenergic mechanisms in stress and anxiety. II. Clinical studies. Synapse. 1996; 23:39–51. [PubMed: 8723134]

Briand LA, Gritton H, Howe WM, Young DA, et al. Modulators in concert for cognition: modulator interactions in the prefrontal cortex. Progress in Neurobiology. 2007; 83:69–91. [PubMed: 17681661]

Bymaster F, Katner J, Nelson D, Hemrick-Luecke S, et al. Atomoxetine increases extracellular levels of norepinephrine and dopamine in the prefrontal cortex of the rat: a potential mechanism for efficacy in attention deficit / hyperactivity disorder. Neuropsychopharmacology. 2002; 27:699–711. [PubMed: 12431845]

Callado L, Meana J, Grijalba B. Selective increase of alpha2-adrenoceptor agonist binding sites in brains of depressed suicide victims. Journal of Neurochemistry. 1998; 70:1114–1123. [PubMed: 9489732]

Charney, D.; Bremner, J.; Redmond, D. Noradrenergic substrates for anxiety and fear. In: Bloom, F.; Kupfer, D., editors. Psychopharmacology: The Fourth Generation of Progress. New York: Raven Press; 1995. p. 387-395.

DeRubeis RJ, Siegle GJ, Hollon SD. Cognitive therapy versus medication for depression: treatment outcomes and neural mechanisms. Nature Reviews Neuroscience. 2008; 9:788–796.

Drevets W, Videen T, Price J, Preskorn S, et al. A functional anatomical study of unipolar depression. Journal of Neuroscience. 1992; 12:3628–3641. [PubMed: 1527602]

Dumartin B, Caille I, Gonon F, Bloch B. Internalization of D1 dopamine receptor in striatal neurons in vivo as evidence of activation by dopamine agonists. Journal of Neuroscience. 1998; 18:1650–1661. [PubMed: 9464990]

Ernst M, Liebenauer L, King A, Fitzgerald G, et al. Reduced brain metabolism in hyperactive girls. Journal of Americon Academy for Child and Adolescent Psychiatry. 1994; 33:858–868.

Frazer A. Norepinephrine involvement in antidepressant action. Journal of Clinical Psychiatry. 2000; 61(Suppl 10):25–30. [PubMed: 10910014]

Fritz JD, Jayanthi LD, Thoreson MA, Blakely RD. Cloning and chromosomal mapping of the murine norepinephrine transporter. Journal of Neurochemistry. 1998; 70:2241–2251. [PubMed: 9603188]

Galli A, DeFelice LJ, Duke BJ, Moore KR, et al. Sodium-dependent norepinephrine-induced currents in norepinephrine-transporter-transfected HEK-293 cells blocked by cocaine and antidepressants. Journal of Experimental Biology. 1995; 198:2197–2212. [PubMed: 7500004]

Garcia AS, Barrera G, Burke TF, Ma S, et al. Autoreceptor-mediated inhibition of norepinephrine release in rat medial prefrontal cortex is maintained after chronic desipramine treatment. Journal of Neurochemistry. 2004; 91:683–693. [PubMed: 15485498]

Glass MJ, Kruzich PJ, Kreek MJ, Pickel VM. Decreased plasma membrane targeting of NMDA-NR1 receptor subunit in dendrites of medial nucleus tractus solitarius neurons in rats self-administering morphine. Synapse. 2004; 53:191–201. [PubMed: 15266550]

Grant M, Weiss J. Effects of chronic antidepressant drug administration and electroconvulsive shock on locus coeruleus electrophysiological activity. Biological Psychiatry. 2001; 49:117–129. [PubMed: 11164758]

Hara Y, Pickel VM. Dendritic distributions of dopamine D1 receptors in the rat nucleus accumbens are synergistically affected by startle-evoking auditory stimulation and apomorphine. Neuroscience. 2007; 146:1593–1605. [PubMed: 17490822]

Hebert C, Habimana A, Elie R, Reader T. Effects of chronic antidepressant treatments on 5-HT and NA transporters in rat brain: an autoradiographic study. Neurochemistry International. 2001; 38:63–74. [PubMed: 10913689]

Huang Y, Maas J, Hu G. The time course of noradrenergic pre- and postsynaptic activity during chronic desipramine treatment. European Journal of Pharmacology. 1980; 68:41–47. [PubMed: 7449833]

Huey ED, Zahn R, Krueger F, Moll J, et al. A psychological and neuroanatomical model of obsessive-compulsive disorder. Journal of Neuropsychiatry and Clinical Neuroscience. 2008; 20:390–408.

Jeannotte AM, McCarthy JG, Redei EE, Sidhu A. Desipramine modulation of alpha-, gamma-synuclein, and the norepinephrine transporter in an animal model of depression. Neuropsychopharmacology. 2009; 34:987–998. [PubMed: 18800064]

Kent J. SNaRIs, NaSSAs, and NaRIs: new agents for the treatment of depression. Lancet. 2000; 355:911–918. [PubMed: 10752718]

Komori K, Kunimi Y, Yamaoka K, Ito T, et al. Semiquantitative analysis of immunoreactivies of tyrosine hydroxylase and aromatic L-amino acid decarboxylase in the locus coeruleus of desipramine-treated rats. Neuroscience Letters. 1992; 147:197–200. [PubMed: 1362806]

Krettek JE, Price JL. The cortical projections of the mediodorsal nucleus and adjacent thalamic nuclei in the rat. Journal of Comparative Neurology. 1977; 171:157–191. [PubMed: 64477]

Lapiz MD, Bondi CO, Morilak DA. Chronic treatment with desipramine improves cognitive performance of rats in an attentional set-shifting test. Neuropsychopharmacology. 2007a; 32:1000–1010. [PubMed: 17077810]

Lapiz MD, Zhao Z, Bondi CO, O'Donnell JM, et al. Blockade of autoreceptor-mediated inhibition of norepinephrine release by atipamezole is maintained after chronic reuptake inhibition. International Journal of Neuropsychopharmacology. 2007b; 10:827–833. [PubMed: 17697440]

Matthies HJ, Han Q, Shields A, Wright J, et al. Subcellular localization of the antidepressant-sensitive norepinephrine transporter. BioMed Central Neuroscience. 2009; 10:65. [PubMed: 19545450]

McMillen B, Warnack W, German D, Shore P. Effects of chronic desipramine treatment on rat brain noradrenergic responses to alpha-adrenergic drugs. European Journal of Pharmacology. 1980; 61:239–246. [PubMed: 6102522]

Meana J, Baruren F, Garcia-Sevilla J. Alpha2-adrenoceptors in the brain of suicide victims: increased receptor density associated with major depression. Biological Psychiatry. 1992; 31:471–490. [PubMed: 1349830]

Michelson D, Adler L, Spencer T, Reimherr F, et al. Atomoxetine in adults with ADHD: two randomized, placebo-controlled studies. Biological Psychiatry. 2003; 53:112–120. [PubMed: 12547466]

Miner, L.; Benmansour, S.; Moore, F.; Blakely, R., et al. 2004 Abstract Viewer/Itinerary Planner. Washington, DC: Society for Neuroscience; 2004. Chronic treatment with a selective serotonin reuptake inhibitor reduces total and plasmalemmal serotonin transporter immunoreactivity in axon terminals within the rat prefrontal cortex.

Miner, L.; Sesack, S. Anatomical Characteristics of Norepinephrine Axons in the Prefrontal Cortex: Unexpected Findings That May Indicate Low Activity State Naïve Animals. In: Tseng, K.; Atzori, M., editors. Monoaminergic Modulation of Cortical Excitability. New York, NY: Springer; 2007. p. 35-65.

Miner LH, Jedema HP, Moore FW, Blakely RD, et al. Chronic stress increases the plasmalemmal distribution of the norepinephrine transporter and the coexpression of tyrosine hydroxylase in norepinephrine axons in the prefrontal cortex. Journal of Neuroscience. 2006; 26:1571–1578. [PubMed: 16452680]

Miner LH, Schroeter S, Blakely RD, Sesack SR. Ultrastructural localization of the serotonin transporter in superficial and deep layers of the rat prelimbic prefrontal cortex and its spatial relationship to dopamine terminals. Journal of Comparative Neurology. 2000; 427:220–234. [PubMed: 11054690]

Miner LH, Schroeter S, Blakely RD, Sesack SR. Ultrastructural localization of the norepinephrine transporter in superficial and deep layers of the rat prelimbic prefrontal cortex and its spatial

relationship to probable dopamine terminals. Journal of Comparative Neurology. 2003; 466:478–494. [PubMed: 14566944]

Moller HJ. Are all antidpressants the same? Journal of Clinical Psychiatry. 2000; 61(Suppl 10):24–27. [PubMed: 10775021]

Moreira FA. Serotonin, the prefrontal cortex, and the antidepressant-like effect of cannabinoids. Journal of Neuroscience. 2007; 27:13369–13370. [PubMed: 18057193]

Mostofsky S, Cooper K, Kates W, Denckla M, et al. Smaller prefrontal and premotor volumes in boys with attention-deficit/hyperactivity disorder. Biological Psychiatry. 2002; 52:785–794. [PubMed: 12372650]

Nelson J. A review of the efficacy of serotonergic and noradrenergic reuptake inhibitors for treatment of major depression. Biological Psychiatry. 1999; 46:1301–1308. [PubMed: 10560035]

Nestler EJ, McMahon A, Sabban EL, Tallman JF, et al. Chronic antidepressant administration decreases the expression of tyrosine hydroxylase in the rat locus coeruleus. Proceedings of the National Academy of Science U S A. 1990; 87:7522–7526.

Ordway GA, Jia W, Li J, Zhu MY, et al. Norepinephrine transporter function and desipramine: residual drug effects versus short-term regulation. J Neurosci Methods. 2005; 143:217–225. [PubMed: 15814154]

Pliszka S, McCracken J, Maas J. Catecholamines in attention-deficit hyperactivity disorder: current prospectives. Journal of Americon Academy for Child and Adolescent Psychiatry. 1996; 35:264–272.

Ramos BP, Arnsten AF. Adrenergic pharmacology and cognition: focus on the prefrontal cortex. Pharmacology & Therapeutics. 2007; 113:523–536. [PubMed: 17303246]

Rauch S, Shin L, Segal E, Pitman R, et al. Selectively reduced regional cortical volumes in post-traumatic stress disorder. Neuroreport. 2003; 14:913–916. [PubMed: 12802174]

Ressler KJ, Mayberg HS. Targeting abnormal neural circuits in mood and anxiety disorders: from the laboratory to the clinic. Nature Neuroscience. 2007; 10:1116–1124.

Riad M, Watkins KC, Doucet E, Hamon M, et al. Agonist-induced internalization of serotonin-1a receptors in the dorsal raphe nucleus (autoreceptors) but not hippocampus (heteroreceptors). Journal of Neuroscience. 2001; 21:8378–8386. [PubMed: 11606626]

Russell V, Allie S, Wiggins T. Increased noradrenergic activity in prefrontal cortex slices of an animals model for attention-deficit hyperactivity disorder - the spontaneously hypertensive rat. Behavioural Brain Research. 2000; 117:69–74. [PubMed: 11099759]

Savchenko V, Sung U, Blakely RD. Cell surface trafficking of the antidepressant-sensitive norepinephrine transporter revealed with an ectodomain antibody. Molecular and Cellular Neuroscience. 2003; 24:1131–1150. [PubMed: 14697674]

Schroeter S, Apparsundaram S, Wiley RG, Miner LH, et al. Immunolocalization of the cocaine- and antidepressant-sensitive l-norepinephrine transporter. Journal of Comparative Neurology. 2000; 420:211–232. [PubMed: 10753308]

Sesack SR, Bressler CN, Lewis DA. Ultrastructural associations between dopamine terminals and local circuit neurons in the monkey prefrontal cortex: a study of calretinin-immunoreactive cells. Neuroscience Letters. 1995; 200:9–12. [PubMed: 8584271]

Singh SK, Yamashita A, Gouaux E. Antidepressant binding site in a bacterial homologue of neurotransmitter transporters. Nature. 2007; 448:952–956. [PubMed: 17687333]

Soares J, Mann J. The functional neuroanatomy of mood disorders. Journal of Psychiatric Research. 1997; 31:393–432. [PubMed: 9352470]

Solanto M. Neuropsychopharmacological mechanisms of stimulant drug action in attention-deficit hyperactivity disorder: a review and integration. Behavioural Brain Research. 1998; 94:127–152. [PubMed: 9708845]

Song L, Kitayama T, Morita K, Morioka N, et al. Down-regulation of norepinephrine transporter expression on membrane surface induced by chronic administration of desipramine and the antagonism by co-administration of local anesthetics in mice. Neurochemistry International. 2008; 52:826–833. [PubMed: 17981365]

Spencer T, Biederman J, Coffey B, Geller D, et al. A double-blind comparison of desipramine and placebo in children and adolescents with chronic Tic disorder and comorbid attention-deficit / hyperactivity disorder. Archives of General Psychiatry. 2002; 59:649–656. [PubMed: 12090818]

Steinbusch HW, Beek A, Frankhuyzen AL, Tonnaer JA, et al. Functional activity of raphe neurons transplanted to the hippocampus and caudate-putamen. An immunohistochemical and neurochemical analysis in adult and aged rats. Annals of the New York Academy of Sciences. 1987; 495:169–184. [PubMed: 3474940]

Svensson T, Udin T. Feedback inhibition of brain noradrenaline neurons by tricyclic antidepressants: alpha-receptor mediation. Science. 1978; 202:1089–1091. [PubMed: 213833]

Szabo S, Blier P. Effect of the selective noradrenergic reuptake inhibitor reboxetine on the firing activity of noradrenaline and serotonin neurons. European Journal of Neuroscience. 2001; 13:2077–2087. [PubMed: 11422448]

Weinshenker D, White SS, Javors MA, Palmiter RD, et al. Regulation of norepinephrine transporter abundance by catecholamines and desipramine in vivo. Brain Research. 2002; 946:239–246. [PubMed: 12137927]

Wolf ME, LeWitt PA, Bannon MJ, Dragovic LJ, et al. Effect of aging on tyrosine hydroxylase protein content and the relative number of dopamine nerve terminals in human caudate. Journal of Neurochemistry. 1991; 56:1191–1200. [PubMed: 1672141]

Zametkin A, Nordahl T, Gross M, King A, et al. Cerebral glucose metabolism in adults with hyperactivity of childhood onset. New England Journal of Medicine. 1990; 323:1361–1366. [PubMed: 2233902]

Zhao Z, Baros AM, Zhang HT, Lapiz MD, et al. Norepinephrine transporter regulation mediates the long-term behavioral effects of the antidepressant desipramine. Neuropsychopharmacology. 2008; 33:3190–3200. [PubMed: 18418364]

Zhou Z, Zhen J, Karpowich NK, Goetz RM, et al. LeuT-desipramine structure reveals how antidepressants block neurotransmitter reuptake. Science. 2007; 317:1390–1393. [PubMed: 17690258]

Zhu CB, Hewlett WA, Feoktistov I, Biaggioni I, et al. Adenosine receptor, protein kinase G, and p38 mitogen-activated protein kinase-dependent up-regulation of serotonin transporters involves both transporter trafficking and activation. Molecular Pharmacology. 2004; 65:1462–1474. [PubMed: 15155839]

Zhu MY, Klimek V, Dilley G, Haycock J, et al. Elevated levels of tyrosine hydroxylase in the locus coeruleus in major depression. Biological Psychiatry. 1999; 46:1275–1286. [PubMed: 10560033]

Zhu MY, Blakely RD, Apparsundaram S, Ordway GA. Down-regulation of the human norepinephrine transporter in intact 293-hNET cells exposed to desipramine. Journal of Neurochemistry. 1998; 70:1547–1555. [PubMed: 9523572]

Zhu MY, Kim CH, Hwang DY, Baldessarini RJ, et al. Effects of desipramine treatment on norepinephrine transporter gene expression in the cultured SK-N-BE(2)M17 cells and rat brain tissue. Journal of Neurochemistry. 2002; 82:146–153. [PubMed: 12091475]

Zhu MY, Ordway GA. Down-regulation of norepinephrine transporters on PC12 cells by transporter inhibitors. Journal of Neurochemistry. 1997; 68:134–141. [PubMed: 8978719]

Zhu MY, Wang WP, Baldessarini RJ, Kim KS. Effects of desipramine treatment on tyrosine hydroxylase gene expression in cultured neuroblastoma cells and rat brain tissue. Brain Research Molecular Brain Research. 2005; 133:167–175. [PubMed: 15710233]

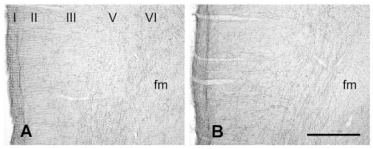

Figure 1.

Coronal sections of the rat PFC showing immunoperoxidase labeling for the mouse anti-NET antibody from vehicle (A) and DMI treated rats (B). Layers are indicated by Roman numerals. Abbreviation: fm, forceps minor. Scale bar = 500 μm.

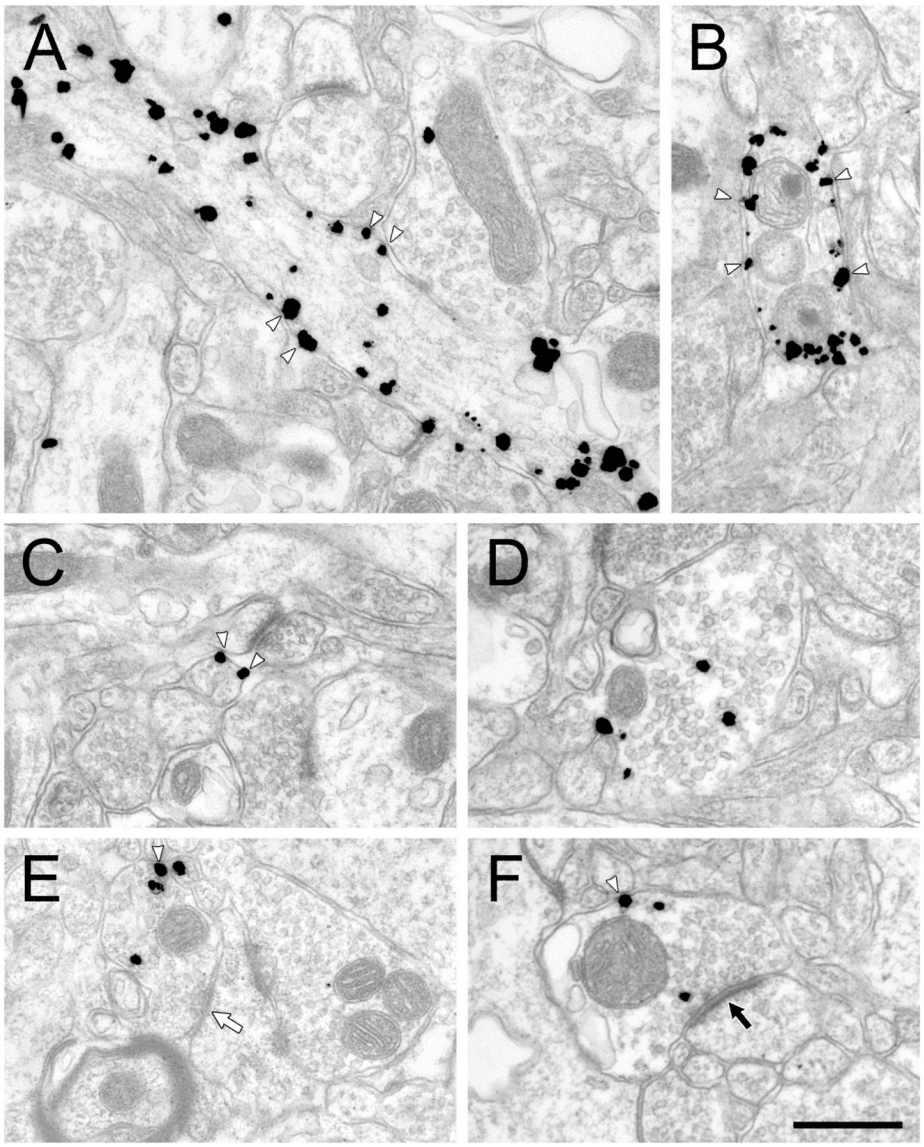

Figure 2.
Electron micrographs showing immunogold-silver labeling for mouse anti-NET in axons in the PFC of rats treated chronically with vehicle. White arrowheads indicate some of the plasma membrane-associated particles. The white arrow in E indicates a symmetric synapse and the black arrow in F indicates an asymmetric synapse. Scale bar = 500 nm.

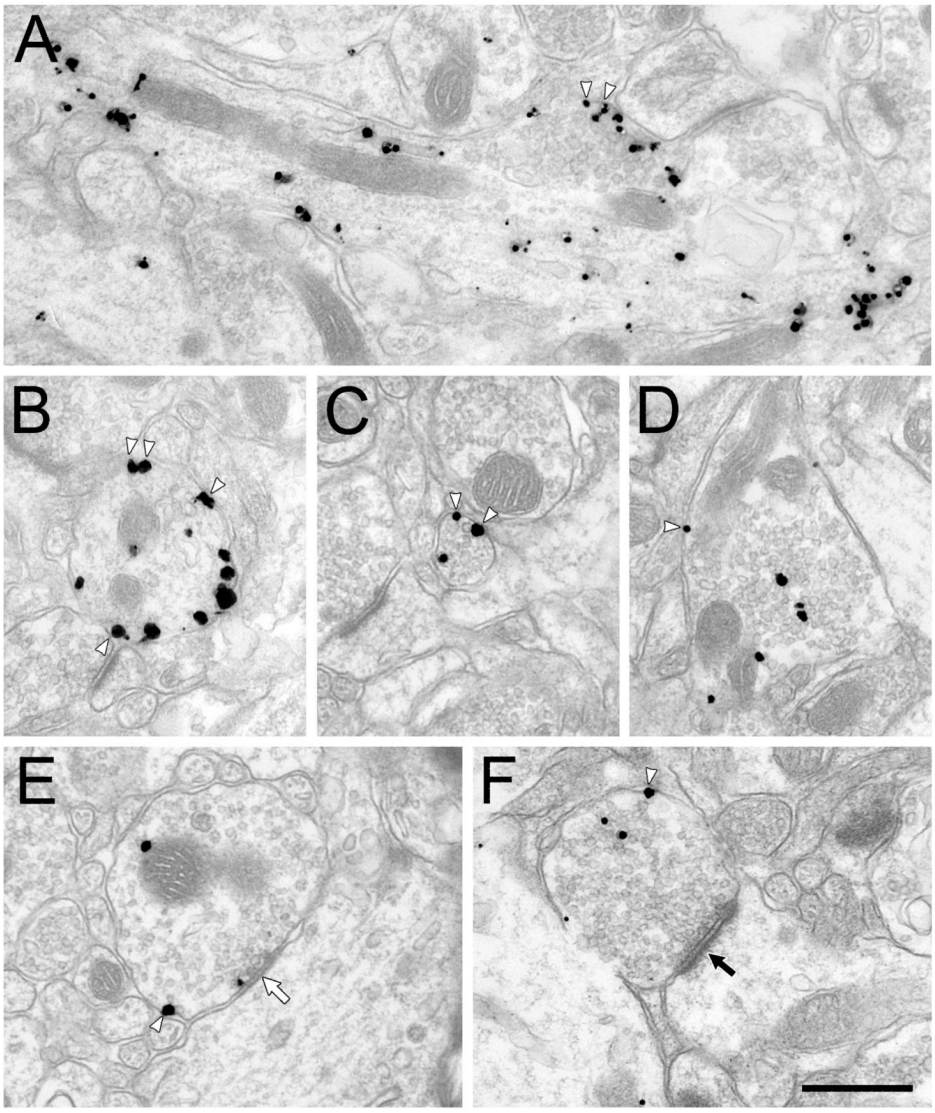

Figure 3.
Electron micrographs showing immunogold-silver labeling for mouse anti-NET in axons in the PFC of rats treated chronically with DMI. White arrowheads indicate some membrane-associated particles. White arrow indicates a symmetric synapse and black arrow indicates an asymmetric synapses. Scale bar = 500 nm.

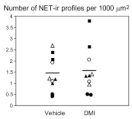

Figure 4.

Quantitative data showing the number of NET-ir profiles per unit tissue area sampled in vehicle and DMI treated rats. Each data point represents one rat. Tissue sections from animals sharing a common symbol were processed at the same time. Black and white symbols indicate tissue processed with the rabbit and mouse anti-NET primary antibodies, respectively. Horizontal bars indicate the group means.

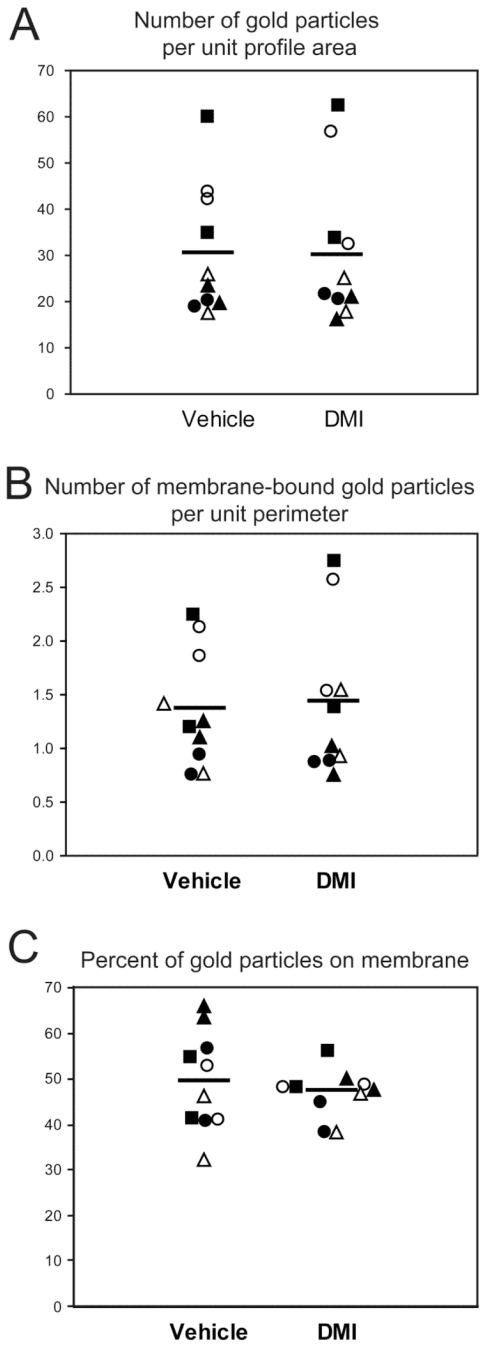

Figure 5.

Quantitative data showing the number of gold particles per unit profile area (A), the number of membrane bound gold particles per unit profile perimeter (B) and the percent of gold particles associated with the plasma membrane (C) in vehicle and DMI treated rats. Each data point represents the mean of approximately 100 NET-ir profiles from one rat. Tissue sections from animals sharing a common symbol were processed at the same time. Black and white symbols indicate tissue processed with the rabbit and mouse anti-NET primary antibodies, respectively. Horizontal bars indicate the group means.

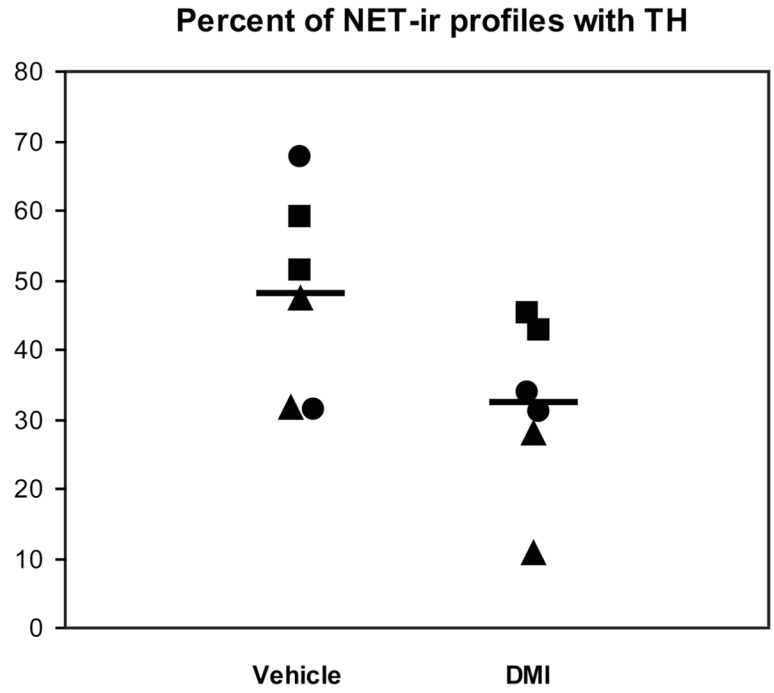

Figure 6.
Quantitative data showing the percent of NET-ir profiles containing detectable immunoperoxidase labeling for TH in DMI treated rats compared to controls. Tissue sections from animals sharing a common symbol were processed at the same time. Horizontal bars indicate the group means.

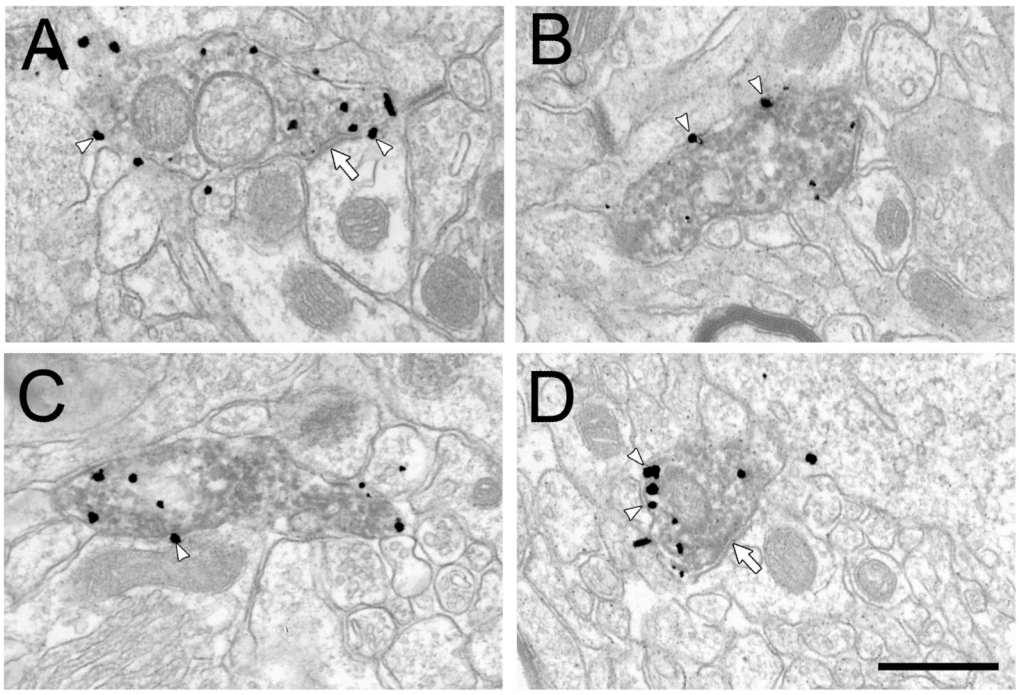

Figure 7.
Electron micrographs from the rat PFC showing the morphological features of dually labeled NET- and TH-ir profiles in vehicle (A,B) and DMI treated rats (C,D). White arrowheads show some of the membrane-associated gold particles and white arrows indicate symmetric synapses. Scale bar = 500 nm.

Table 1

Plasma DMI Levels and Sampling Summary

Treatment	Cohort	Animal	Plasma DMI (ng/ml)	# NET-ir profiles	Tissue area (um^2)
Vehicle	A	1		134	55,987
	A	2		130	62,974
	B	3		102	244,419
	B	4		99	196,830
	C	5		111	94,041
	C	6		129	128,712
	D	7		160	59,516
	D	8		110	90,629
	E	9		116	105,909
	E	10		126	65,085
				1,217	1,104,103
DMI	A	1	506.60	110	41,550
	A	2	497.00	143	37,616
	B	3	139.00	119	234,942
	B	4	643.00	121	258,503
	C	5	113.00	125	93,195
	C	6	777.00	112	84,272
	D	7	162.08	106	111,916
	D	8	170.97	127	90,192
	E	9	156.87	108	52,605
	E	10	211.63	99	92,379
			337.72	1,170	1,097,171

Table 2

95% Confidence Limits

Dependent measure	Estimated Ratio	Lower limit	Upper limit
#NET/unit tissue area	1.032	0.79	1.36
# Gold/unit profile area	0.988	0.79	1.24
Membrane gold/unit perimeter	0.995	0.88	1.12
% gold on membrane	0.932	0.81	1.07
% synapses	1.176	0.90	1.54
% TH	0.662	0.45	0.98

The numbers listed in the Estimated Ratio column are the ratios of drug mean values to control mean values in this study.

Table 3

Synaptic Contacts Formed by NET-ir Profiles in the Rat PFC

					Postsynaptic target		
Treatment	**Primary antibody**	**# NET-ir profiles**	**# Synapses (%)**	**# Symmetric (%)**	**Dendrite**	**Spine**	**Soma**
Vehicle	rabbit	697	79 (11)	25 (32)	24	54	1
	mouse	513	94 (18)	23 (24)	26	67	
DMI	rabbit	725	107 (15)	33 (31)	28	78	
	mouse	462	85 (18)	14 (16)	22	63	